

Evaluation of Neutron Radiography Reactor LEU-Core Start-Up Measurements

John D. Bess,* Thomas L. Maddock, Andrew T. Smolinski, and Margaret A. Marshall

*Idaho National Laboratory
P.O. Box 1625, MS 3855, Idaho Falls, Idaho 83415*

Abstract—Benchmark models were developed to evaluate the cold-critical start-up measurements performed during the fresh core reload of the neutron radiography (NRAD) reactor with low-enriched uranium fuel. Experiments include criticality, control rod worth measurements, shutdown margin, and excess reactivity for four core loadings with 56, 60, 62, and 64 fuel elements. The worths of four graphite reflector block assemblies and an empty dry tube used for experiment irradiations were also measured and evaluated for the 60-fuel-element core configuration. Dominant uncertainties in the experimental k_{eff} come from uncertainties in the manganese content and impurities in the stainless steel fuel cladding as well as the ^{236}U and erbium poison content in the fuel matrix. Calculations with MCNP5 (Monte Carlo N-Particle version 5-1.60) and ENDF/B-VII.0 neutron nuclear data are $\sim 1.4\%$ (9σ) greater than the benchmark model eigenvalues, which is commonly seen in Monte Carlo simulations of other TRIGA (Training, Research, Isotopes, General Atomics) reactors. Simulations of the worth measurements are within the 2σ uncertainty for most of the benchmark experiment worth values. The complete benchmark evaluation details are available in the 2014 edition of the International Handbook of Evaluated Reactor Physics Benchmark Experiments.

I. INTRODUCTION

The neutron radiography (NRAD) reactor is a 250-kW TRIGA (Training, Research, Isotopes, General Atomics) Mark II tank-type research reactor¹ at the Idaho National Laboratory (INL). It is primarily utilized for indirect neutron radiography analysis of both irradiated and unirradiated fuels and materials. The NRAD reactor is a conversion-type reactor that was originally located at the Puerto Rico Nuclear Center and converted to a TRIGA-FLIP-(Fuel Life Improvement Program)-fueled system (70% ^{235}U) in 1971. The 2-MW Puerto Rico research reactor was closed in 1976; a portion of the reactor was then moved in 1977 and rebuilt as the NRAD reactor (shown in Fig. 1) (Ref. 2).

The Reduced Enrichment for Research and Test Reactors Program, in support of the Global Threat

Reduction Initiative, required conversion of all civilian reactor facilities from highly enriched uranium (HEU) to low-enriched uranium (LEU) fuel (<20% ^{235}U) (Ref. 3). The NRAD reactor core was completely defueled, and refueling with LEU began in September 2009; start-up testing after the HEU-to-LEU fuel conversion of the NRAD TRIGA reactor was performed between March and June 2010, with a core loading of 60 fuel elements. Because the core excess reactivity (ER) was lower than originally predicted and would not allow for extended operations, the NRAD reactor core was later upgraded via the addition of four fuel elements and four graphite elements. Start-up measurements for the upgraded NRAD core were performed in April 2013.

Complete benchmark evaluation reports for the initial start-up measurements⁴ and the final upgraded core⁵ are available in the *International Handbook of Evaluated Reactor Physics Benchmark Experiments*⁶ (IRPhEP Handbook). The initial benchmark report for the start-up

*E-mail: john.bess@inl.gov

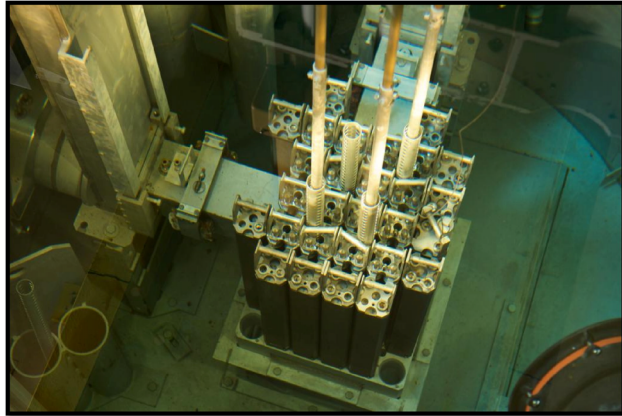


Fig. 1. In-tank view of the NRAD reactor core (60-fuel-element loading).

60-fuel-element critical configuration has been revised since its initial release⁷ to include rod worth measurements and evaluation of the 56-fuel-element core.⁸ Additional revisions include an updated fuel composition and associated uncertainties as well as inclusion of water saturation in the graphite blocks of the reflector assemblies.

II. OVERVIEW OF LEU CORE CONVERSION MEASUREMENTS

The NRAD reactor is composed of fuel in three- and four-element clusters that can be arranged in a variety of lattice patterns, depending on reactor performance requirements. A schematic of a four-element cluster assembly is shown in Fig. 2. The grid plate consists of 36 holes, in a 6×6 rectangular pattern, that mate with the end fittings of the fuel cluster assemblies. The final upgraded core configuration (see Fig. 3) contains 64 fuel elements, four graphite elements, two water-followed shim control rods, and one water-followed regulating rod. A water hole is provided as an experimental irradiation position via an empty control rod guide tube located near the core center. An aluminum “dry tube” can be inserted into the southwest corner of the core to serve as an additional irradiation location. Unclad nuclear-grade graphite blocks provide peripheral neutron reflection. Two beam lines extend from the midplane of the core on the north and east sides; each services a radiography station.

The aluminum grid plate is bolted to a support structure, which is in turn bolted to a mounting pad and the water-filled reactor tank. The fuel is a mixture of uranium, erbium, and zirconium hydride. The uranium is enriched to ~ 19.75 wt% in ^{235}U and is ~ 30 wt% of the fuel. The fuel meat contains a uniform dispersion of 0.9 wt% natural erbium, a burnable poison, which is used to offset the initial reactivity of the fresh fuel. The hydrogen-to-zirconium ratio is 1.58, and the “spine” of the fuel is a

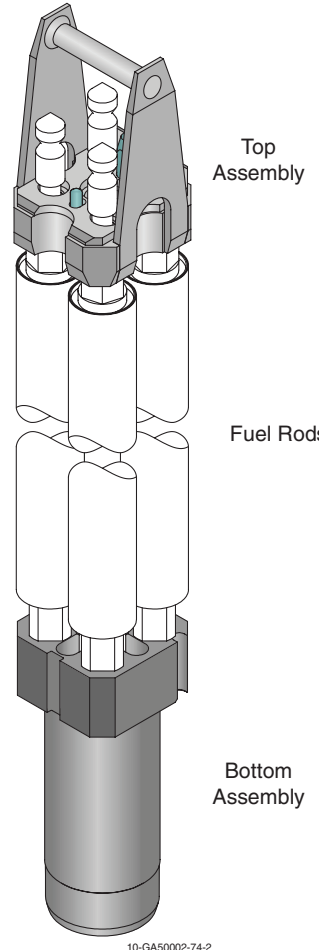


Fig. 2. Four-fuel-element cluster assembly.

solid zirconium rod. The fuel, a molybdenum poison disk, and two axial, nuclear-grade graphite reflectors are all clad within a stainless steel tube and end fittings, as shown in Fig. 4. The boron carbide control rods are clad in aluminum. The graphite elements use identical cladding and fittings as the fuel elements but contain only graphite rods with the same composition as the axial graphite reflectors found in the fuel elements.

Typical operation of the NRAD reactor involves full withdrawal of the two shim control rods a total of 38.1 cm (15 in.) with criticality maintained by adjusting core reactivity with the regulating control rod position. Initial criticality was achieved with 56 fuel elements. Three additional critical configurations were obtained with loadings of 60, 62, and finally 64 fuel elements. Control rod worth measurements, core ER, and shutdown margin (SDM) were determined for each core loading, where the control rod worths are measured directly, and the ERs and SDMs were derived from the control rod worth measurements. The reactivity worths of four graphite reflector block assemblies were also measured, as well

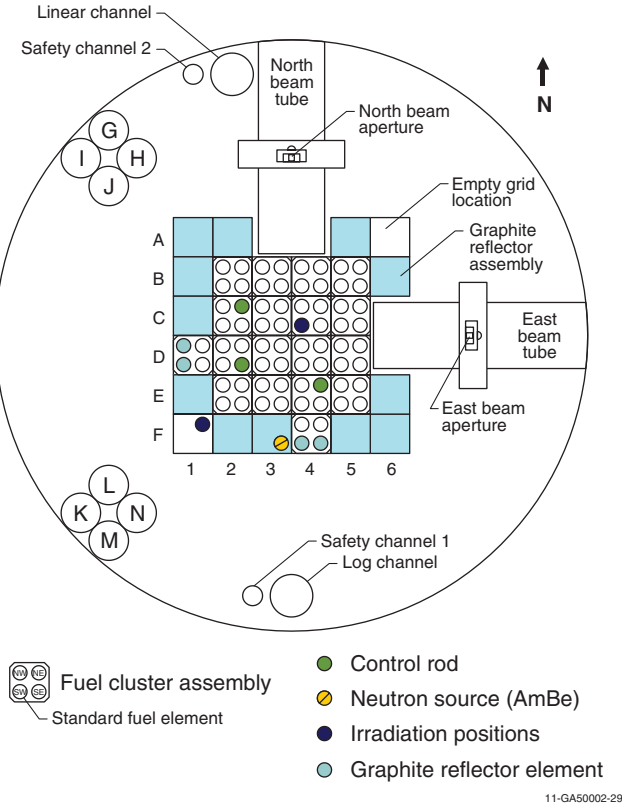


Fig. 3. NRAD reactor LEU core schematic (64-fuel-element loading).

as the worth of the empty dry tube, but only for the 60-fuel-element core configuration. All these zero-power measurements were evaluated as acceptable benchmark experiments.

Additional power calorimetric and core ER measurements were performed at the full operational power of 250 kW for the 60- and 64-fuel-element core loadings. These measurements, however, have not been evaluated.

III. UNCERTAINTY IN THE EXPERIMENTAL k_{eff}

Extensive effort was made to fully characterize as many reactor core details as possible. Manufacturing drawings were gathered from storage and incorporated in model design and analyses. As-built fuel element data include dimensional measurements, compositions, and impurities. A spare fuel element was deconstructed and sampled for further detailed analysis of the impurity content of the fuel, zirconium, molybdenum, graphite, and steel. Samples of a spare graphite block were used to determine the density and impurity content of the graphite reflectors. Two in-core graphite reflector block assemblies and a dry graphite reflector block assembly were weighed to assess the amount of water saturation in the graphite blocks.

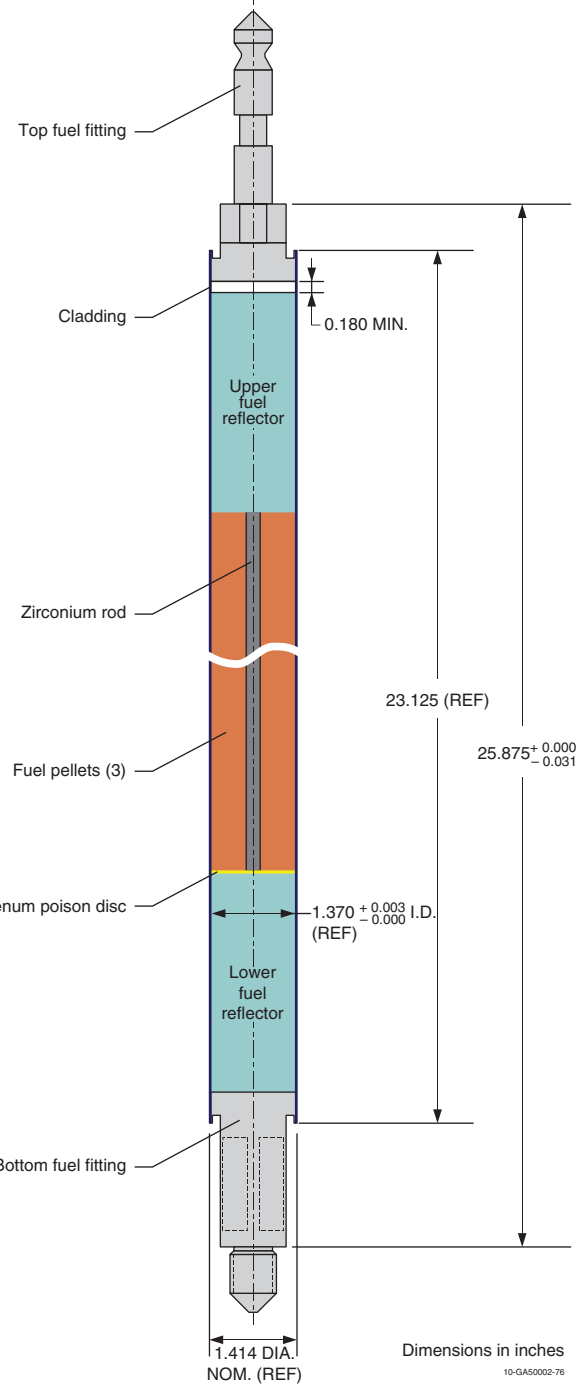


Fig. 4. Typical TRIGA fuel element.

Perturbation analyses were performed using models of the NRAD reactor core (see Sec. IV) to evaluate the effective uncertainty in the experimental k_{eff} values. The computational analysis of the uncertainties was performed using the Monte Carlo N-Particle version 5-1.60 (MCNP5) code⁹ with ENDF/B-VII.0 nuclear data.¹⁰ A summary of the significant evaluated uncertainties and the total experimental uncertainty in k_{eff} is provided in Table I

TABLE I
Summary of Experimental Uncertainties*

Parameter\Number of fuel elements	56	60	62	64
Mass of ^{235}U in fuel	18	18	18	18
^{234}U content in fuel	29	31	27	30
^{236}U content in fuel	43	46	49	48
Hydrogen-to-zirconium ratio in fuel	19	18	19	18
Erbium content in fuel	50	49	49	50
Manganese content in steel clad	71	68	65	70
Nickel content in steel clad	17	14	20	12
Impurities in steel clad	36	35	36	42
Impurities in boron carbide absorber	19	10	10	10
Graphite reflector block density	14	12	14	11
Graphite reflector block dimensions	14	14	19	15
Water saturation of graphite blocks	19	Negligible	Negligible	17
Assembly pitch in grid plate	16	18	15	17
Diameter of assembly holes in grid	13	14	12	13
Impurities in tank water	26	10	10	10
Placement of beam lines	11	14	12	Negligible
Total experimental uncertainties	122 (0.163 \$)	116 (0.155 \$)	116 (0.155 \$)	120 (0.160 \$)

*In pcm.

while a thorough discussion of the uncertainty evaluation is provided in the benchmark reports.^{4,5}

A comprehensive uncertainty analysis was initially performed for the 60-fuel-element core configuration to evaluate the impact of the numerous geometric, material, and measurement uncertainties upon k_{eff} . The simulated critical condition of the core is relatively insensitive to many of the evaluated uncertainty perturbations in the reactor parameters. A consolidated uncertainty evaluation was performed for the remaining three core configurations that accounted solely for uncertainties contributing at least 10 pcm to the total experimental uncertainty in k_{eff} of the 60-fuel-element core configuration.

The dominant uncertainties include the manganese content in the stainless steel cladding, the impurity content in the cladding, the erbium content of the fuel, and the ^{236}U content of the fuel. Type 304 stainless steel has a manganese content up to 2 wt%; the benchmark model of the NRAD reactor uses a content of 1 wt% and a bounding uncertainty with uniform probability distribution of ± 1 wt% divided by $\sqrt{3}$ to represent a 1σ normal distribution uncertainty. The impurity content of the steel was measured using glow discharge mass spectrometry. Many of the impurities were reported to be below the detection limit, and an uncertainty in the measured values was unavailable. A bounding uncertainty of $\pm 100\%$ of the reported content was evaluated and similarly reduced to a 1σ value. The average erbium content across the 64 fuel elements is 0.90 ± 0.02 wt% (1σ), and the average ^{236}U content is 0.22 ± 0.09 wt% (1σ). The total experimental uncertainty is ~ 120 pcm in each core configuration.

Perturbation analyses were not performed to evaluate the uncertainty in the reactivity effects measurements. Experimental measurement uncertainties were typically greater in magnitude than those obtained by evaluating the perturbation of system parameters (i.e., uncertainties in geometries and compositions) using computational methods.

IV. BENCHMARK MODEL DEVELOPMENT

Detailed models of the NRAD reactor core configurations were prepared to evaluate simplification biases applied to the benchmark models. Many of the model simplifications produced small or negligible biases. Furthermore, homogenization of many of the model details, such as assembly fittings, grid plate, and other support structures, similarly resulted in small or negligible bias effects and could thus be removed from the benchmark models. A comprehensive bias analysis was performed only for the 60-fuel-element core configuration. The various simplifications were evaluated individually to determine their effective contribution as a model bias and/or bias uncertainty. The square root of the sum of the squares of the bias uncertainties was selected to represent the total bias uncertainty, 90 pcm (0.12 \$), in all four benchmark model critical configurations. The experiment and bias uncertainties are combined in quadrature to obtain a benchmark model uncertainty of ~ 150 pcm (0.20 \$).

A midplane view of the benchmark model for the 64-fuel-element core configuration is shown in Fig. 5, with

the vertical alignment of the core components provided in Fig. 6. Axial profiles of the fuel elements and control rods are shown in Fig. 6, with additional fuel element detail provided in Fig. 7. The minor impurities in the various reactor components were removed from the models as part of the bias assessment. The graphite reflector blocks are fully saturated with water at 37 vol %. The density of the tank water was modeled based on the measured experimental temperature during each of the cold-critical conditions.

The eigenvalue and additional parameters were calculated using MCNP5 and ENDF/B-VII.0 nuclear data. Additional calculated parameters were gathered from the Monte Carlo analysis (MCNP5 with ENDF/B-VII.0) of the benchmark model for the 64-fuel-element core: neutron leakage, fission fractions by energy, fission fractions by isotope, average number of neutrons produced per fission (\bar{v}), energy of average neutron lethargy causing fission, neutron generation time, and effective delayed neutron fraction. The neutron generation time and the effective delayed neutron fraction were calculated using the adjoint capabilities in MCNP; neutron leakage represents the leakage of neutrons from the benchmark model. Results are included in Table II. The calculated eigenvalues are $\sim 1.4\%$ ($\sim 1.75 \pm 9\sigma$) greater

than the benchmark model k_{eff} values. Calculations of the eigenvalue using MCNP5 with ENDF/B-VII.0 nuclear data for the Slovenian TRIGA reactor benchmark¹¹ are also higher than the benchmark experiment values. Similar computational biases in eigenvalue calculations were also reported for the TRIGA Mark II reactor at the Musashi Institute of Technology¹² and the converted LEU core of the University of Wisconsin Nuclear Reactor.¹³ More recent investigations in Slovenia have isolated problems with the ENDF/B-VII.0 nuclear data library. The highest contributors to the overprediction of k_{eff} are due to cross-section data for ^{91}Zr and the thermal scattering data, $S(\alpha, \beta)$, for hydrogen and zirconium in the ZrH lattice. The study concluded that the higher elastic scattering resonance integral increases thermal neutron flux by improving neutron thermalization, leading to higher fission rates and consequently increasing k_{eff} ; this effect is more pronounced in smaller critical systems.¹⁴

V. EVALUATION OF WORTH MEASUREMENTS

The benchmark model summarized in Sec. IV was used in calculations of the 25 reactivity effects measurements: control rod worths (12), ER (4), SDM (4),

TABLE II
Comparison of Benchmark Experiment (k_E) and Calculated (k_C)
Eigenvalues Using MCNP5 with ENDF/B-VII.0 Nuclear Data

Number of Fuel Elements	Calculated	Benchmark	$\frac{k_C - k_E}{k_E} (\%)$
	$k_C \pm \sigma$	$k_E \pm \sigma$	
56	1.01412 ± 0.00007	1.0012 ± 0.0015	1.29
60	1.01413 ± 0.00007	1.0012 ± 0.0015	1.29
62	1.01459 ± 0.00007	1.0011 ± 0.0015	1.35
64	1.01479 ± 0.00007	1.0012 ± 0.0015	1.36
Additional Calculated Parameters for 64-Fuel-Element Core Configuration			
Neutron Balance (%)		Leakage Capture (n, xn) Fission	2.11 56.36 0.05 41.48
Fission fraction, by energy (%)		Thermal (<0.625 eV) Intermediate Fast (> 100 keV)	80.68 16.33 2.99
Fission fraction, by isotope (%)		^{234}U ^{235}U ^{236}U ^{238}U	0.01 98.74 0.01 1.24
Average number of neutrons produced per fission Energy of average neutron lethargy causing fission (MeV) Neutron generation time (μs) Effective delayed neutron fraction			2.444 0.264 24.23 0.00754

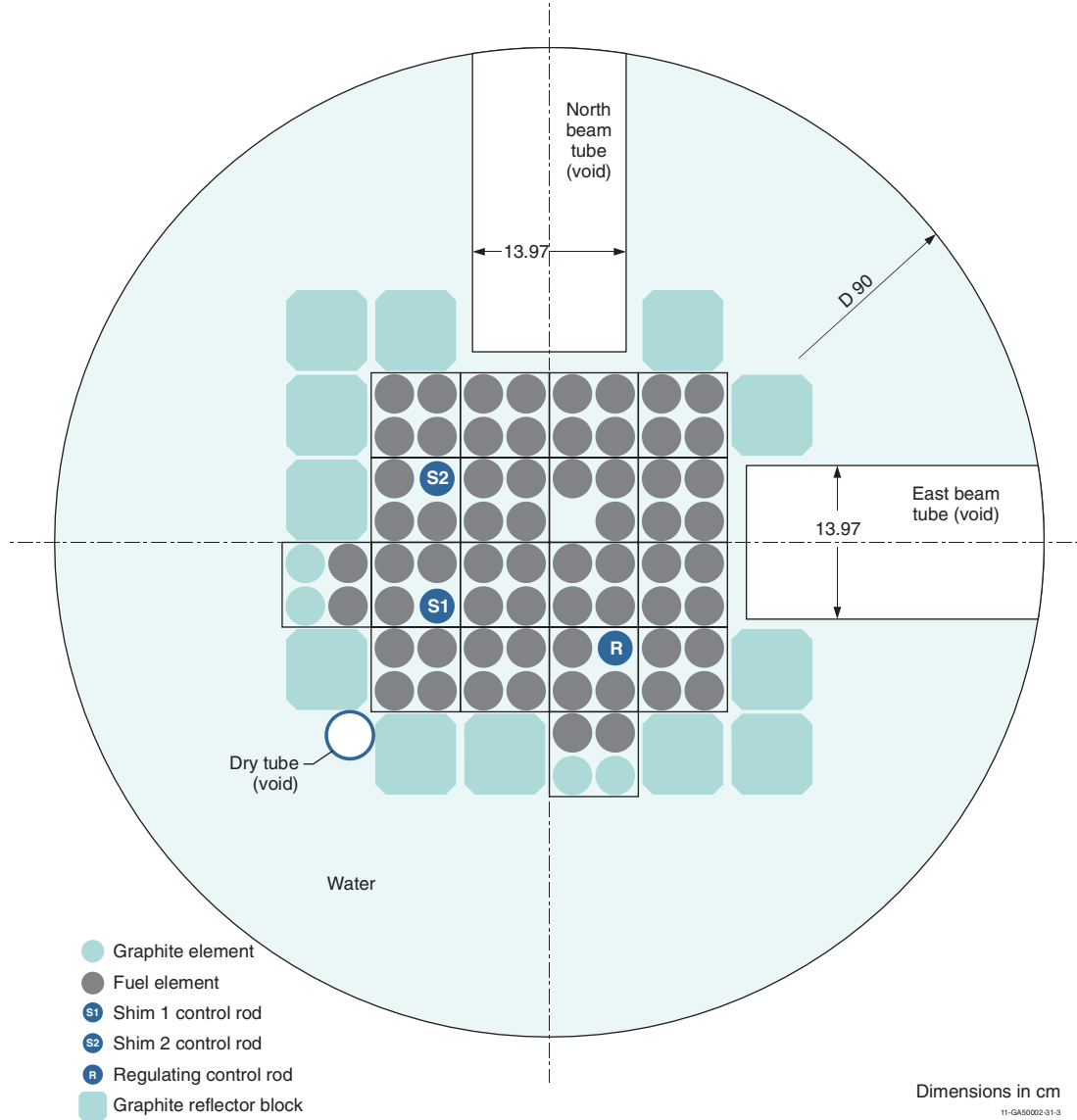


Fig. 5. Midplane cross-section view of 64-fuel-element benchmark model. Position of the dry tube is shown although it was not inserted for the critical configuration.

graphite reflector block worths (4), and dry tube worth (1). Reactivity measurements performed during the NRAD reactor start-up measurements were typically reported in absolute values. The convention taken in this paper is the use of negative values for reporting measurements that reduce multiplication properties of the system via absorption (control rods, SDM, reflector block removal, and dry tube insertion) and positive values for effects that then increase k_{eff} (ER). Reactivity worths for NRAD measurements are typically reported in dollars or cents.

Historically, a delayed neutron fraction value β_{eff} of 0.0071 was used to convert reactivity measurements to and from Δk . General Atomics utilizes a β_{eff} value of 0.0078 in its design analysis of the NRAD reactor.

Reported values for β_{eff} in TRIGA-type reactors have been known to range between 0.0070 and 0.0080 (Refs. 15 through 18). Typically, the delayed neutron fraction is insensitive to reflector material.¹⁶ Calculations using various contemporary nuclear data libraries, and also using both the prompt method and adjoint-weighted point kinetics, were performed to assess the variability in β_{eff} . A median value of 0.0075 ± 0.0004 (5%, 1σ) was selected for both benchmark and calculated reactivity effects measurements for the NRAD reactor; reported β_{eff} values from open literature can similarly be utilized to estimate a mean value of 0.0075. Further details regarding this analysis can be found in the benchmark evaluation reports.^{4,5} The uncertainty in β_{eff} is included in the

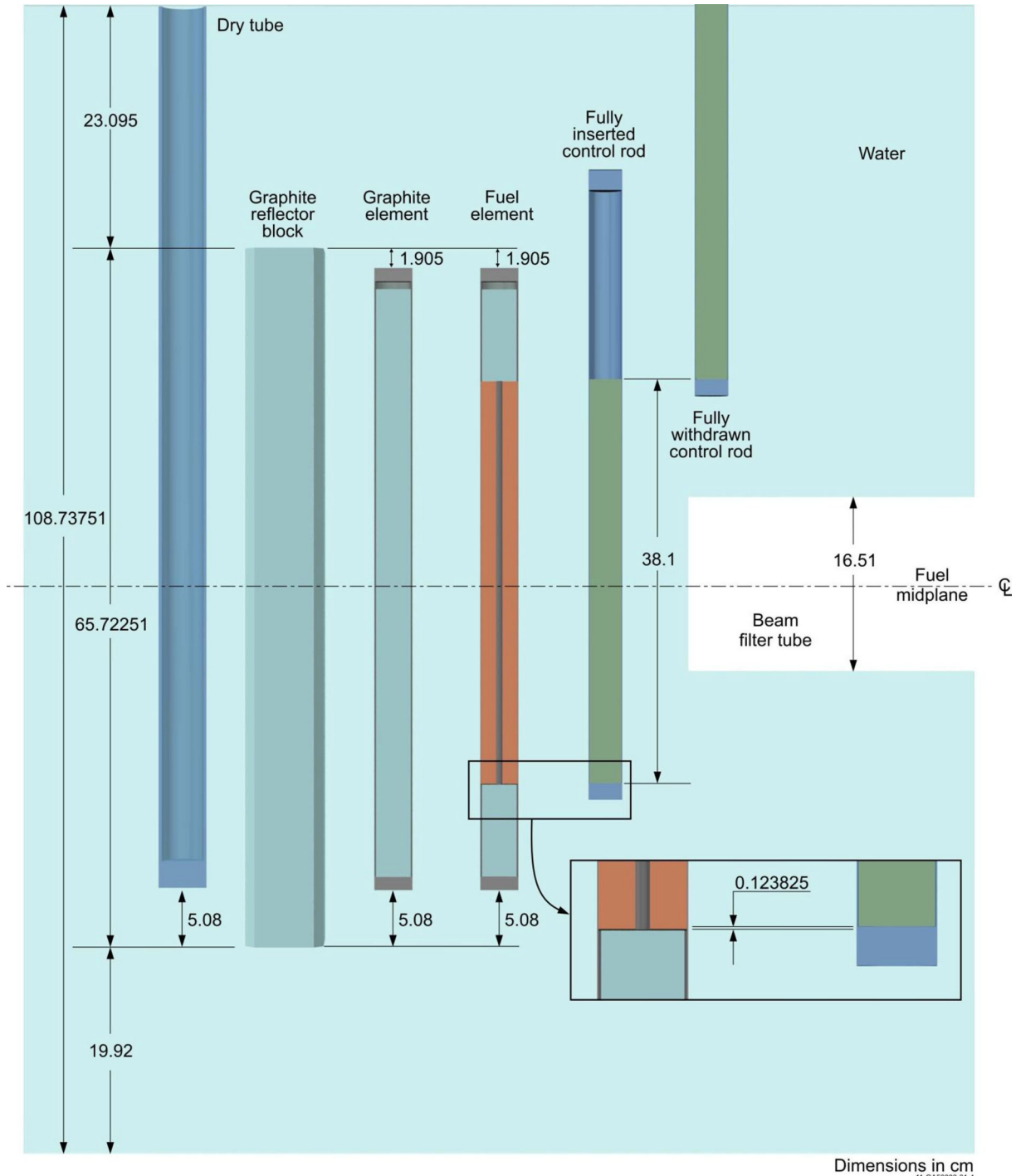


Fig. 6. Vertical placement of benchmark model components.

uncertainty propagation of all worth calculations and measurements and is considered to be of sufficient magnitude to encompass the range of β_{eff} values either calculated or found in open literature.

Measurement uncertainties were not reported. Rod drop measurements were performed to determine the

worth of the shim control rods and withdrawn worth of the regulating control rod. Rod drops in a critical reactor generate short-lived flux modes uncharacteristic of the system's fundamental mode. Rod drop measurements, however, are performed and measured on the timescale of minutes, when these system harmonics are considered

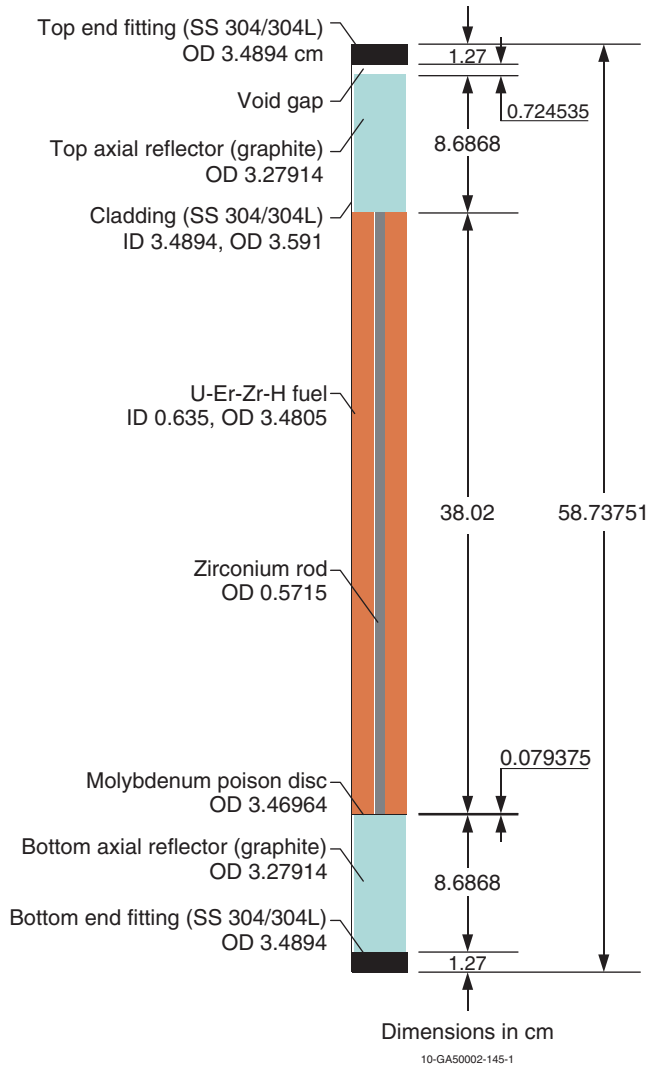


Fig. 7. Benchmark model TRIGA fuel element.

negligible.¹⁹ The prompt rod drop method is the easiest means to estimate the reactivity change in a reactor core because it is based on the prompt flux adjustment occurring directly after the perturbation of the core state and assumes that the delayed neutron source is unchanged. However, this method is sensitive to spatial effects and less accurate than other methods. Typical uncertainties are on the order of 5% to 6% for a TRIGA reactor.²⁰ Uncertainties in the rod drop technique of the MASURCA reactor have also been reported on the order of 5% to 6% (Ref. 21). Typical uncertainties in rod insertion methods include uncertainties in the delayed neutron data, which is systematic and common to all measuring methods. Source redistribution in the flux of the subcritical core leads to rod shadowing effects where the positions of the control rods in the reactor impact the worth of the rod being measured. The uncertainty for rod insertion methods in TRIGA reactors has been reported

elsewhere as 3% to 5% for individual rod worths, with a statistical error of <0.2%. However, the impact of rod shadowing effects increases the estimated uncertainty to ~10% (Ref. 22). Measurements implementing driven rod insertion methods, very similar to the rod drop method, demonstrated rod shadowing effects impacting the measured control rod worth by >30%. On average, however, the reported values varied by ~8% (Ref. 23). The NRAD reactor typically operates with the two shim rods fully withdrawn. A comparison of two regulating rod measurements was performed: one with the shim rods partially inserted and a full regulating rod drop and the other with the shim rods fully withdrawn to obtain a partial rod drop worth, and then positive period measurements to obtain the worth of the inserted portion of the regulating rod. The difference between these two measurements was ~7% of the worth of the regulating rod. An uncertainty of 10% was selected to represent the uncertainty in the rod drop measurement method for the NRAD reactor.

Positive period measurements, also known as the rod exchange method, where the rod worth is measured relative to another, calibrated, control rod, were used to determine the worth of the inserted portion of the regulating rod and ER of each core configuration. The ER is defined as the core reactivity present with all control elements withdrawn from the core.²⁴ Multiple measurement steps were taken, on the order of ≤ 20 ϕ /step, until the regulating rod was fully withdrawn. The shim rod positions are adjusted as a pair to compensate for the change in reactivity and return the core to a critical state. Calibration curve measurements in a TRIGA reactor have shown that the uncertainties in positive period measurements are slightly less than 10% and include uncertainties in control rod positions, rod shadowing effects, and statistical errors.²² Because of severe local flux distribution deformation in these types of measurements, often simulations need to model the individual measurement steps to calculate the total measured rod worth. An uncertainty of 10% is typical for this type of measurement²⁵ and has been used as a standard for treating the uncertainty in reactivity measurements in other TRIGA reactors.¹² An uncertainty of 10% was selected to represent the uncertainty in the positive period measurement method for the NRAD reactor.

The total worth of the regulating control rod is the combination of the inserted worth measured using the positive period technique and the withdrawn worth measured using the rod drop technique. The uncertainties in the single rod drop measurement and multiple positive period measurements were propagated to obtain an uncertainty in the total rod worth. The SDM is defined as the negative reactivity of the core present when all control elements have been fully inserted to achieve minimum core multiplication.²⁴ It is simply calculated as the sum of the withdrawn control rod worths or,

alternatively, as the total worth of all control rods minus the remaining in-core control rod worth, which is, in this case, the core ER. The uncertainty in the worth measurements is combined in quadrature to obtain the uncertainty in the SDM.

The worths of the graphite reflector block assemblies were ascertained experimentally by measuring the core ER of the nominal 60-fuel-element core configuration and comparing it against the ER measured for the core with a given graphite assembly removed. Graphite reflector assemblies in positions A-5, C-1, D-1, and F-4 (grid positions shown in Fig. 3) were individually assessed. It should be noted that in the 60-fuel-element core configuration, the graphite reflector assembly in position A-1 was originally located in position D-1 and the assembly in position F-6 was in position F-4. The dry tube worth was experimentally determined by comparing the regulating rod positions for the core both with and without the dry tube present and deducing its effective worth.

Reactivity measurements were simulated with control rod movements. The benchmark models for these measurements are based on the rod movements and core configurations performed in the actual experiments. Worth calculations, also performed with MCNP5 and ENDF/B-VII.0, either directly mimicked benchmark model rod movements (method 1) or were more simply modeled with all control rods fully withdrawn from the core and comparing rod worth measurements against this configuration (method 2), effectively ignoring rod shadowing effects in the calculations because the uncertainty due to rod shadowing was already incorporated in the uncertainty of the benchmark experiment worths. Shim rod worth simulations employed the benchmark method of dropping a fully withdrawn shim rod from the benchmark critical configuration or alternatively dropped from a core model where all three control rods were fully withdrawn. The regulating rod worth simulations either repeated the partial rod drop and positive period measurements or alternatively dropped from a state with all three control rods fully withdrawn from the core. The SDM was obtained by summing the dropped rod worth of the two shim rods and the partially withdrawn regulating rod or alternatively by comparing the subcritical state with all control rods fully inserted against the critical configuration to assess a worth. The ER was obtained via simulation of the positive period measurements or alternatively by comparing the supercritical state with all control rods fully withdrawn against the critical configuration. The worth of the graphite reflector blocks was simulated via the measurement method of comparing core ERs between the nominal critical configuration and the critical configuration when a graphite assembly was removed completely from the core; alternatively, a given graphite assembly was removed from the critical core configuration, and the worth difference was calculated without any movement of control

rod positions. The dry tube worth is simply calculated by comparing the 60-fuel-element critical configuration both with and without the dry tube.

The benchmark experiment reactivity worths ρ_E for the various reactivity effects measurements are compared with the calculated worths ρ_C in Table III ($\beta_{eff} = 0.0075$). The Monte Carlo statistical uncertainty in the worth calculations is $\sim 0.01 \pm$; the 5% uncertainty in β_{eff} is also applied to the total uncertainty in the calculated reactivity worths. Calculations of the shim and regulating rods are within 2σ of the benchmark values. Simulation of the rod worths using either method produces acceptable results. Results for the SDM are within 1σ using method 1 but are up to 3σ higher than the benchmark values when using method 2. Except for the 60-fuel-element core configuration, which is high by $\sim 5\sigma$ for method 1, calculations for ER are within 2σ using either of the simulation methods. The cause for the discrepancy in the core with 60 fuel elements is unknown. Calculation of the graphite reflector block assembly worth is high but within 3σ for method 1; overprediction of core ER for the various 60-fuel-element core configurations appears to contribute to this discrepancy. Calculation of the block worth using method 2 is within 1σ for all four positions. Calculation of the dry tube worth is in excellent agreement with the benchmark experiment value.

VI. CONCLUSIONS

Benchmark models were developed to evaluate the cold-critical start-up measurements performed during the fresh core reload of the NRAD reactor with LEU fuel. Experiments include criticality, control rod worths, SDM, and ER for four core loadings. The worths of four graphite reflector block assemblies and an empty dry tube used for experiment irradiations were measured and evaluated for the 60-fuel-element core configuration. Dominant uncertainties in the experimental k_{eff} come from uncertainties in the manganese and impurity contents of the stainless steel fuel cladding and the erbium and ^{236}U content in the fuel matrix. Calculations with MCNP5 and ENDF/B-VII.0 nuclear data are $\sim 1.4\%$ (9σ) greater than the benchmark model eigenvalues, which is a problem common in other TRIGA reactor simulations most likely due to Zr and ZrH cross-section data. Simulations of the worth measurements are within the 3σ uncertainty for most of the benchmark experiment worths. The benchmark reports are available in the 2014 edition of the IRPhEP Handbook; further revisions, if necessary, will be included in future handbook releases.

ACKNOWLEDGMENTS

The authors would like to thank L. Montierth, N. Zhang, A. M. Phillips, K. Schreck, B. Briggs, and E. Woolstenhulme

EVALUATION OF NEUTRON RADIOPHYSICS REACTOR

 TABLE III
 Comparison of Benchmark and Calculated Reactivity Worth Measurements

Number of Fuel Elements	Measurement	Method	Calculated	Benchmark	ρ_C/ρ_E
			$\rho (\$) \pm \sigma$	$\rho (\$) \pm \sigma$	
56	Shim rod 1	1	-3.01 ± 0.15	-2.76 ± 0.31	1.09
		2	-2.94 ± 0.15		1.07
	Shim rod 2	1	-2.57 ± 0.13	-2.72 ± 0.30	0.94
		2	-2.47 ± 0.12		0.91
	Regulating rod	1	-2.59 ± 0.11	-2.43 ± 0.23	1.07
		2	-2.57 ± 0.13		1.06
	SDM	1	-7.76 ± 0.23	-7.54 ± 0.49	1.03
		2	-8.73 ± 0.44		1.16
60	ER	1	0.41 ± 0.03	0.37 ± 0.02	1.11
		2	0.40 ± 0.02		1.08
	Shim rod 1	1	-2.84 ± 0.14	-2.68 ± 0.30	1.06
		2	-2.70 ± 0.14		1.01
	Shim rod 2	1	-2.65 ± 0.13	-2.75 ± 0.33	0.96
		2	-2.35 ± 0.12		0.85
	Regulating rod	1	-2.60 ± 0.11	-2.42 ± 0.16	1.07
		2	-2.62 ± 0.13		1.08
62	SDM	1	-6.75 ± 0.23	-6.73 ± 0.47	1.00
		2	-7.15 ± 0.36		1.06
	ER	1	1.34 ± 0.04	1.12 ± 0.05	1.20
		2	1.19 ± 0.06		1.06
	Block A-5	1	-0.30 ± 0.07	-0.17 ± 0.06	1.76
		2	-0.15 ± 0.01		0.88
	Block C-1	1	-0.56 ± 0.06	-0.41 ± 0.06	1.37
		2	-0.44 ± 0.03		1.07
64	Block D-1	1	-0.56 ± 0.06	-0.43 ± 0.06	1.30
		2	-0.47 ± 0.03		1.09
	Block F-4	1	-0.61 ± 0.06	-0.45 ± 0.06	1.36
		2	-0.39 ± 0.02		0.87
	Dry tube	1	-0.06 ± 0.01	-0.06 ± 0.01	1.00
		2			
	Shim rod 1	1	-2.85 ± 0.14	-2.66 ± 0.30	1.07
		2	-2.63 ± 0.13		0.99
62	Shim rod 2	1	-2.57 ± 0.13	-2.66 ± 0.30	0.97
		2	-2.20 ± 0.11		0.83
	Regulating rod	1	-2.58 ± 0.07	-2.49 ± 0.12	1.04
		2	-2.60 ± 0.13		1.04
	SDM	1	-6.37 ± 0.20	-6.24 ± 0.43	1.02
		2	-6.72 ± 0.34		1.08
	ER	1	1.63 ± 0.05	1.56 ± 0.06	1.04
		2	1.65 ± 0.08		1.06
64	Shim rod 1	1	-3.13 ± 0.16	-2.92 ± 0.33	1.07
		2	-2.79 ± 0.14		0.96
	Shim rod 2	1	-2.87 ± 0.14	-2.94 ± 0.33	0.98
		2	-2.30 ± 0.12		0.78
	Regulating rod	1	-2.54 ± 0.06	-2.45 ± 0.08	1.04
		2	-2.47 ± 0.12		1.01
	SDM	1	-6.21 ± 0.21	-6.06 ± 0.47	1.02
		2	-6.26 ± 0.31		1.03
	ER	1	2.32 ± 0.05	2.24 ± 0.08	1.04
		2	2.25 ± 0.11		1.00

from INL; J. Bolin and A. Vega from General Atomics; and R. McKnight and R. Lell from Argonne National Laboratory for their review and support in developing a comprehensive benchmark evaluation. Additional gratitude is expressed to C. White from INL for generating graphical representations. Further appreciation is expressed to all the international participants in the International Reactor Physics Experiment Evaluation Project for all their well-spent time and effort. This paper was prepared at INL for the U.S. Department of Energy under contract DE-AC07-05ID14517.

REFERENCES

1. D. M. FOUQUET, J. RAZVI, and W. L. WHITTEMORE, "TRIGA Research Reactors: A Pathway to the Peaceful Applications of Nuclear Energy," *Nuclear News*, **46**, 12, 46 (2003).
2. A. A. WEEKS, D. P. PRUETT, and C. C. HEIDEL, "Modifications to the NRAD Reactor (1977 to Present)," *Proc. 10th U.S. TRIGA User's Conf.*, College Station, Texas, April 7–9, 1986.
3. C. LANDERS, "Reactors Identified for Conversion, Reduced Enrichment for Research and Test Reactors (RERTR) Program," *Proc. RERTR 2005 Int. Mtg. Reduced Enrichment for Research and Test Reactors*, Boston, Massachusetts, November 6–10, 2005.
4. J. D. BESS, T. L. MADDOCK, and M. A. MARSHALL, "Fresh-Core Reload of the Neutron Radiography (NRAD) Reactor with Uranium(20)-Erbium-Zirconium-Hydride Fuel," NRAD-FUND-RESR-001, Rev. 2, *International Handbook of Evaluated Reactor Physics Benchmark Experiments*, NEA/NSC/DOC(2006)1, Organisation for Economic Co-operation and Development/Nuclear Energy Agency (2014).
5. J. D. BESS, "Neutron Radiography (NRAD) Reactor 64-Element Core Upgrade," NRAD-FUND-RESR-002, *International Handbook of Evaluated Reactor Physics Benchmark Experiments*, NEA/NSC/DOC(2006)1, Organisation for Economic Co-operation and Development/Nuclear Energy Agency (2014).
6. *International Handbook of Evaluated Reactor Physics Benchmark Experiments*, NEA/NSC/DOC(2006)1, Organisation for Economic Co-operation and Development/Nuclear Energy Agency (2014).
7. J. D. BESS, T. L. MADDOCK, and M. A. MARSHALL, "Benchmark Evaluation of the NRAD Reactor LEU Core Startup Measurements," *Proc. Int. Conf. Nuclear Criticality (ICNC) 2011*, Edinburgh, Scotland, September 19–23, 2011.
8. J. D. BESS and M. A. MARSHALL, "Additional Benchmark Evaluation of the NRAD Reactor LEU Core Conversion," *Trans. Am. Nucl. Soc.*, **106**, 861 (2012).
9. X-5 MONTE CARLO TEAM, "MCNP—A General N-Particle Transport Code, Version 5, Vol. I: Overview and Theory," LA-UR-03-1987, Los Alamos National Laboratory (2003, updated 2005).
10. M. B. CHADWICK et al., "ENDF/B-VII.0: Next Generation Evaluated Nuclear Data Library for Nuclear Science and Technology," *Nucl. Data Sheets*, **107**, 2931 (2006); <http://dx.doi.org/10.1016/j.nds.2006.11.001>.
11. R. JERAJ and M. RAVNIK, "TRIGA Mark II Reactor: U(20)—Zirconium Hydride Fuel Rods in Water with Graphite Reflector," IEU-COMP-THERM-003, *International Handbook of Evaluated Criticality Safety Benchmark Experiments*, NEA/NSC/DOC(95)03, Organisation for Economic Co-operation and Development/Nuclear Energy Agency (2010).
12. T. MATSUMOTO and N. HAYAKAWA, "Benchmark Analysis of TRIGA Mark II Reactivity Experiment Using a Continuous Energy Monte Carlo Code MCNP," *J. Nucl. Sci. Technol.*, **37**, 1082 (2000); <http://dx.doi.org/10.1080/18811248.2000.9714995>.
13. K. T. AUSTIN, "LEU Core Design for the Conversion of University of Wisconsin Nuclear Reactor," *Proc. RERTR 2010 Int. Mtg. Reduced Enrichment for Research and Test Reactors*, Lisbon, Portugal, October 10–13, 2010.
14. L. SNOJ et al., "Testing of Cross Section Libraries on Zirconium Benchmarks," *Ann. Nucl. Energy*, **42**, 71 (2012); <http://dx.doi.org/10.1016/j.anucene.2011.12.001>.
15. A. TRKOV et al., "Reactivity Measurements in a Close-to-Critical TRIGA Reactor Using a Digital Reactivity Meter," *Kerntechnik*, **57**, 296 (1992).
16. M. T. SIMNAD, F. C. FOUSHÉE, and G. B. WEST, "Fuel Elements for Pulsed TRIGA® Research Reactors," *Nucl. Technol.*, **28**, 31 (1976); <http://dx.doi.org/10.13182/NT76-2>.
17. L. SNOJ et al., "Calculation of Kinetic Parameters for Mixed TRIGA Cores with Monte Carlo," *Ann. Nucl. Energy*, **37**, 223 (2010); <http://dx.doi.org/10.1016/j.anucene.2009.10.020>.
18. T. MATSUMOTO, "Benchmark Analysis of Criticality Experiments in the TRIGA Mark II Using a Continuous Energy Monte Carlo Code MCNP," *J. Nucl. Sci. Technol.*, **35**, 662 (1998); <http://dx.doi.org/10.1080/18811248.1998.9733922>.
19. T. WILLIAMS, M. ROSSELET, and W. SCHERER, "Critical Experiments and Reactor Physics Calculations for Low-Enriched High Temperature Gas Cooled Reactors," IAEA-TEC-DOC-1249, International Atomic Energy Agency (2001).
20. C. JAMMES et al., "Comparison of Reactivity Estimations Obtained from Rod-Drop and Pulsed Neutron Source Experiments," *Ann. Nucl. Energy*, **32**, 1131 (2005); <http://dx.doi.org/10.1016/j.anucene.2005.02.013>.
21. G. PERRET et al., "Determination of Reactivity by a Revised Rod-Drop Technique in the MUSE-4 Programme—Comparison with Dynamic Measurements," *Proc. 7th Information Exchange Mtg. Actinide and Fission Product Partitioning and Transmutation*, Jeju, Korea, October 14–16, 2002.

EVALUATION OF NEUTRON RADIOGRAPHY REACTOR

22. I. MELE, M. RAVNIK, and A. TRKOV, "TRIGA Mark II Benchmark Experiment, Part II: Pulse Operation," *Nucl. Technol.*, **105**, 52 (1994); <http://dx.doi.org/10.13182/NT94-1>.
23. A. TRKOV et al., "Application of the Rod-Insertion Method for Control Rod Worth Measurements in Research Reactors," *Kerntechnik*, **60**, 255 (1995).
24. J. J. DUDERSTADT and L. J. HAMILTON, *Nuclear Reactor Analysis*, John Wiley and Sons, Ann Arbor, Michigan (1976).
25. R. JERAJ, B. GLUMAC, and M. MAUČEC, "Monte Carlo Simulation of the TRIGA Mark II Benchmark Experiment," *Nucl. Technol.*, **120**, 179 (1997); <http://dx.doi.org/10.13182/NT97-1>.